Available online at www.sciencedirect.com
ScienceDirect
Tunnelling and Underground Space Technology 22 (2007) 230–237
Tunnelling and Underground Space Technology incorporating Trenchless Technology Research
www.elsevier.com/locate/tust

Technical note

Ground reaction analyses in conventional tunnelling excavation

Z. Guan [a,*], Y. Jiang [b], Y. Tanabasi [b]

[a] Department of Civil Engineering, Graduate School of Science and Technology, Nagasaki University, 1-14 Bunkyo Machi, Nagasaki 852-8521, Japan
[b] Department of Civil Engineering, Nagasaki University, Nagasaki 852-8521, Japan

Received 14 March 2006; received in revised form 13 June 2006; accepted 15 June 2006
Available online 6 September 2006

Abstract

Based on the axial symmetrical plane strain assumption, given that the rock mass satisfies the Mohr–Coulomb failure criterion and exhibits strain-softening behavior, this paper represents two categories of theoretical methods for ground reaction analyses in conventional tunnelling excavation. They distinguish from each other according to their treatments for plastic strain: one is the simplified method in terms of total plastic strain (i.e. does not consider the unloading process of ground), the other is the rigorous method in terms of incremental plastic strain (i.e. takes the unloading process into account). Although the philosophies of these two categories of theoretical methods have been proposed by former researchers, the discrepancy between them has never been noticed and reported. Through case studies, this paper highlights the discrepancy quantitatively, estimates the maximum error caused by the simplified method, and further discusses their applicability.

Keywords: Ground reaction curve; Strain-softening behavior; Unloading process; Total plastic strain; Incremental plastic strain

1. Introduction

Estimation of the support required to stabilize a tunnel opening during excavation, especially in the vicinity of the tunnel face, is essentially a four-dimensional problem. It not only concerns with three spatial dimensions but also another temporal dimension, which corresponds to the advancing process of the tunnel face (or synonymously the unloading process of ground). The Convergence confinement method (CCM) represents a classic and effective tool for the support system design in conventional tunnelling, which compromises the complex nature with a general albeit simplified approach. It consists of three basic components: longitudinal deformation profile (LDP), support characteristic curve (SCC) and ground reaction curve (GRC). The arrangement and intersection of these three curves are considered, to account for the complex nature near the tunnel face compactly and effectively.

Numerous papers have been contributed to this topic during its several decades of development, and a comprehensive review of CCM has been reported recently by Carranza-Torres and Fairhurst (2000). The LDP, which presents the radial displacement that occurring along the axis of an unsupported tunnel, is generally evaluated by monitoring data in site or by 3D numerical simulations (e.g. Panet and Guenot, 1982; Tonon and Amadei, 2002). The SCC, which describes the relationship between the inner pressure carried by supports and the radial displacement at tunnel wall, allow one to take different types of supports, pre-released displacement before supporting and other support-related characteristics into account, (e.g. Oreste, 2003; Graziani et al., 2005).

The GRC, which describes the relationship between the decreasing of inner pressure and the increasing of radial displacement of tunnel wall, is generally evaluated by theoretical methods, such as analytical or semi-analytical elasto-plastic analyses based on axial symmetry plane strain assumption. These available methods, although distinguished from different failure criterions and different post-failure behaviors, can be generally divided into two

* Corresponding author. Tel.: +81 95 8192612; fax: +81 95 8192627.
E-mail address: guanzc@gel.civil.nagasaki-u.ac.jp (Z. Guan).

0886-7798/$ - see front matter © 2006 Elsevier Ltd. All rights reserved.
doi:10.1016/j.tust.2006.06.004

categories according to their treatments for plastic strain. One is the simplified method in terms of total plastic strain, and is represented by Brown et al. (1983), Oreste and Peila (1996), Jiang et al. (2001) and others. The other is the rigorous method in terms of incremental plastic strain, and is represented by Detournay (1986), Carranza-Torres and Fairhurst (1999), Alonso et al. (2003) and others.

However, the discrepancy between these two categories of method has not been reported yet. In this paper, therefore, given that rock mass satisfies the Mohr–Coulomb failure criterion and exhibits strain-softening behavior, these two categories of theoretical methods are derived respectively. For the simplified one, analytical solutions are available, whereas only semi-analytical solutions can be obtained for the rigorous one. The significant difference in theory assumption between them is revealed in this paper, and the discrepancy between them is highlighted quantitatively through case studies. Moreover, the applicability of them is also discussed.

2. Problem description

For universality, the rock mass is assumed to exhibit strain-softening behavior in this paper, which can be reduced into a perfect elasto-plastic one or an elasto-brittle one in some special cases (e.g. Jiang, 1993; Hudson and Harrison, 1997). Although many researchers have reported that strain-softening materials may experience instability and bifurcation during an unloading process (e.g. Hill, 1950; Varas et al., 2005), this paper restricts the discussion to its stable (or basic) solutions.

Generally, the rock mass exhibiting strain-softening behavior is characterized by a transitional failure criterion $f(\sigma_{ij},\eta)$ and a plastic potential $g(\sigma_{ij},\eta)$. η is a softening parameter controlling the gradual transition from a peak failure criterion (or potential) to a residual one. In this paper, the rock mass is assumed to satisfy the linear Mohr–Coulomb criterion and linear plastic potential. As for the softening parameter, it can be defined in different ways, but so far there has not been a common accepted one among researchers. In this paper, the major principal plastic strain $\varepsilon_1^{\mathrm{p}}$ is employed as the softening parameter, because it is relatively simple and can be obtained easily from the results of uniaxial compression tests (schematically represented in Fig. 1). Therefore, the failure criterion f and the plastic potential g can be formulated as follows according to uniaxial compression tests.

$$f = \sigma_1 - K_{\mathrm{p}}\sigma_3 - \sigma_{\mathrm{c}} = \begin{cases} \sigma_1 - K_{\mathrm{p}}\sigma_3 - \left(\sigma_{\mathrm{c}}^1 + \frac{(\sigma_{\mathrm{c}}^1-\sigma_{\mathrm{c}}^2)\varepsilon_1^{\mathrm{p}}}{\alpha\varepsilon_{1e}}\right) & (0 \leqslant \varepsilon_1^{\mathrm{p}} \leqslant \alpha\varepsilon_{1e}) \\ \sigma_1 - K_{\mathrm{p}}\sigma_3 - \sigma_{\mathrm{c}}^2 & (\varepsilon_1^{\mathrm{p}} \geqslant \alpha\varepsilon_{1e}) \end{cases} \quad (1)$$

$$g = \sigma_1 - K_\psi\sigma_3 = \begin{cases} \sigma_1 - K_\psi^1\sigma_3 & (0 \leqslant \varepsilon_1^{\mathrm{p}} \leqslant \alpha\varepsilon_{1e}) \\ \sigma_1 - K_\psi^2\sigma_3 & (\varepsilon_1^{\mathrm{p}} \geqslant \alpha\varepsilon_{1e}) \end{cases} \quad (2)$$

Here, K_{p} is the passive coefficient, and remains unchanged within the complete plastic region. σ_{c} is the compression strength, and transits gradually from σ_{c}^1 to σ_{c}^2, according to the evolution of the major principal plastic strain $\varepsilon_1^{\mathrm{p}}$. K_ψ is the dilation factor, and equals to K_ψ^1 and K_ψ^2 for softening region and residual region, respectively.

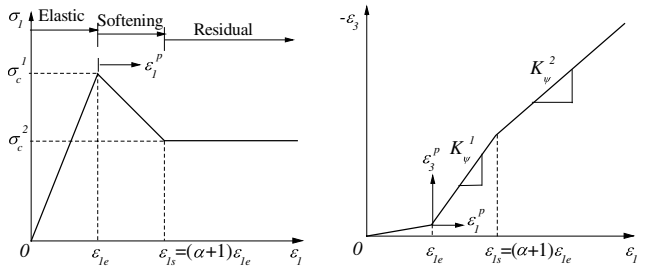

Fig. 1. Strain-softening behaviors of rock sample in uniaxial compression tests.

The excavation of a long deep tunnel with circular cross section under a hydrostatic in situ stress condition can be considered as an axial symmetry plane strain problem, while neglecting the influence of gravity, and restricting the out-of-plane principal stress as intermediate stress. The basic assumptions are the same with the conventional CCM presented in aforementioned papers., the geomechanics sign convention (i.e. compression and contraction are taken as positive) is used in this paper, and the radial displacement towards tunnel axis is taken as positive consequently.

After tunnel excavation, the surrounding rock mass will experience elastic, softening and residual regions sequentially, according to different fictitious inner pressure provided by the tunnel face and the support. For universality, Fig. 2 schematically represents a universal case in the presence of three regions. In Fig. 2, P_0 is the hydrostatic in situ stress; P_{i} is the fictitious inner pressure; R_{a}, R_{s} and R_{e}, are the radii of the tunnel opening, the softening–residual (S–R) interface and the elastic–softening (E–S) interface, respectively. The objective is to evaluate the stress and displacement redistributions (or namely ground responses) after excavation, which is presented in next section.

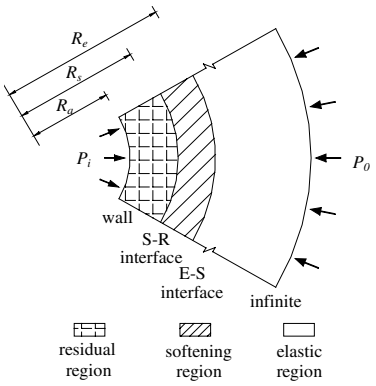

Fig. 2. Schematic representation of the rock mass states after excavation.

3. Ground responses analyses

3.1. Analyses in elastic region

The elastic solution for the excavation of cylindrical cavities in a hydrostatic ally loaded medium is given by Lame's solution (e.g. Timoshenko and Goodier, 1970). It applies to the elastic region of this problem (where $r > R_e$ in Fig. 2), and the stresses and displacement distributions in this region can be expressed as

$$\sigma_r = P_0 - (P_0 - \sigma_{re})\frac{R_e^2}{r^2}, \quad \sigma_\theta = P_0 + (P_0 - \sigma_{re})\frac{R_e^2}{r^2} \tag{3}$$

$$\varepsilon_r = -\frac{(P_0 - \sigma_{re})}{2G}\frac{R_e^2}{r^2}, \quad \varepsilon_\theta = \frac{(P_0 - \sigma_{re})}{2G}\frac{R_e^2}{r^2} \tag{4}$$

$$u = \frac{(P_0 - \sigma_{re})}{2G}\frac{R_e^2}{r} \tag{5}$$

Here, σ_r and σ_θ are the stresses in radial and tangential directions; ε_r and ε_θ are the strains in radial and tangential directions; u is the radial displacement, the unique degree of spatial freedom in this problem. G is the shear modulus of rock mass, and σ_{re} denotes the radial stress at the E–S interface.

On the other hand, the radial and tangential stresses at the E–S interface ($r = R_e$) should verify the Mohr–Coulomb criterion Eq. (1) exactly, which leads to:

$$\sigma_{re} = \frac{2P_0 - \sigma_c^1}{K_p + 1}, \quad \sigma_{\theta e} = 2P_0 - \frac{2P_0 - \sigma_c^1}{K_p + 1} \tag{6}$$

An important feature of this solution is that the stresses at the E–S interface are known constants and independent of the interface position. Similarly, the strains at this interface have the same feature as shown in Eq. (7). This position-independent feature forms the basis of affine transformation, which will simplify the analyses in plastic region significantly

$$\varepsilon_{re} = -\frac{(P_0 - \sigma_{re})}{2G}, \quad \varepsilon_{\theta e} = \frac{(P_0 - \sigma_{re})}{2G} \tag{7}$$

3.2. Analyses in plastic region

3.2.1. Affine transformation

An affine transformation proposed by Detournay (1986) is introduced first, which simplifies the analyses in plastic region significantly. Since the states at the E–S interface are known constant and position-independent, R_e can serve as a minified scale to map the physical plane into a unit plane, by the affine transformation formulated as Eq. (8). Correspondingly, all the mechanical variables such as stress, strain and displacement in the physical plane can also be normalized into their dimensionless counterparts in the unit plane (denoted by tilde mark), according to Eqs. (9)

$$\rho = \frac{r}{R_e} \tag{8}$$

$$\tilde{\sigma}(\rho) = \frac{1}{P_0 - \sigma_{re}}\sigma(r, R_e) \tag{9.1}$$

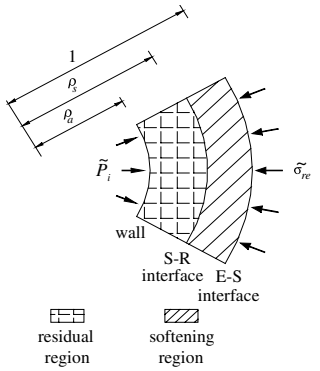

Fig. 3. Schematic representation of the plastic region in the unit plane.

$$\tilde{\varepsilon}(\rho) = \frac{2G}{P_0 - \sigma_{re}}\varepsilon(r, R_e) \tag{9.2}$$

$$\tilde{u}(\rho) = \frac{2G}{R_e(P_0 - \sigma_{re})}u(r, R_e) \tag{9.3}$$

Fig. 3 schematically illustrates the plastic region in the unit plane, corresponding to its counterpart shown in Fig. 2. In Fig. 3, ρ_a, ρ_s and 1 are the radii of the tunnel wall, the softening–residual (S–R) interface and the elastic-softening (E–S) interface in the unit plane, respectively. $\tilde{\sigma}_{re}$ is the normalized radial stress at E–S interface, and $\tilde{P}_i$ is the normalized inner pressure at tunnel wall.

In addition, the partial derivatives of all mechanical variables with respect to r and R_e are evaluated with the following operators:

$$\frac{\partial(\,)}{\partial r} = \frac{1}{R_e}\frac{\mathrm{d}(\,)}{\mathrm{d}\rho}, \quad \frac{\partial(\,)}{\partial R_e} = -\frac{\rho}{R_e}\frac{\mathrm{d}(\,)}{\mathrm{d}\rho} \tag{10}$$

Meanwhile, the normalized states at the E-S interface ($\rho = 1$) are greatly simplified into constants as follows. They serve as the boundary conditions for further analyses in the softening region

$$\tilde{\sigma}_r(1) = \tilde{\sigma}_{re} \tag{11.1}$$

$$\tilde{\varepsilon}_r(1) = \tilde{\varepsilon}_{re} = -1, \quad \tilde{\varepsilon}_\theta(1) = \tilde{\varepsilon}_{\theta e} = 1 \tag{11.2}$$

$$\tilde{u}(1) = \tilde{u}_e = 1 \tag{11.3}$$

Similarly, the failure criterion and the plastic potential are also transformed and simplified in terms of normalized mechanical variables. Notice that the major and minor stresses (or strains) correspond to the tangential and radial stresses (or strains) in this problem

$$\tilde{f} = \tilde{\sigma}_\theta - K_p\tilde{\sigma}_r - \tilde{\sigma}_c = \begin{cases} \tilde{\sigma}_\theta - K_p\tilde{\sigma}_r - \left(\tilde{\sigma}_c^1 + \frac{(\tilde{\sigma}_c^1 - \tilde{\sigma}_c^2)\tilde{\varepsilon}_\theta^p}{\alpha}\right) & (0 \leqslant \tilde{\varepsilon}_\theta^p \leqslant \alpha) \\ \tilde{\sigma}_\theta - K_p\tilde{\sigma}_r - \tilde{\sigma}_c^2 & (\tilde{\varepsilon}_\theta^p \geqslant \alpha) \end{cases} \tag{12}$$

$$\tilde{g} = \tilde{\sigma}_\theta - K_\psi\tilde{\sigma}_r = \begin{cases} \tilde{\sigma}_\theta - K_\psi^1\tilde{\sigma}_r & (0 \leqslant \tilde{\varepsilon}_\theta^p \leqslant \alpha) \\ \tilde{\sigma}_\theta - K_\psi^2\tilde{\sigma}_r & (\tilde{\varepsilon}_\theta^p \geqslant \alpha) \end{cases} \tag{13}$$

3.2.2. Plastic analyses in terms of total plastic strain

The analyses in terms of total plastic strain assume that the total plastic strains consist of a constant elastic part and an increasing plastic part, as formulated by Eq. (14). The relationship between the tangential and radial plastic strains can be obtained from plastic potential and flow rule, as formulated by Eq. (15). Actually, these two equations can be obtained directly from stress–strain relationship shown in Fig. 1. The displacement–strain relationship is rather simple by virtue of axial symmetry and is formulated by Eq. (16)

$$\tilde{\varepsilon}_r = \tilde{\varepsilon}_{re} + \tilde{\varepsilon}_r^p, \quad \tilde{\varepsilon}_\theta = \tilde{\varepsilon}_{\theta e} + \tilde{\varepsilon}_\theta^p \tag{14}$$

$$\tilde{\varepsilon}_r^p = -K_\psi \tilde{\varepsilon}_\theta^p \tag{15}$$

$$\tilde{\varepsilon}_r = \frac{d\tilde{u}}{d\rho}, \quad \tilde{\varepsilon}_\theta = \frac{\tilde{u}}{\rho} \tag{16}$$

The association of these three equations leads to the displacement compatibility equation in the softening region:

$$\frac{d\tilde{u}}{d\rho} + K_\psi^1 \frac{\tilde{u}}{\rho} = \tilde{\varepsilon}_{re} + K_\psi^1 \tilde{\varepsilon}_{\theta e} = K_\psi^1 - 1 \tag{17}$$

Solving the differential equation with its boundary condition $\tilde{u}(1) = 1$, the distribution of the normalized displacement in this region can be expressed as Eq. (18), and further, the normalized tangential plastic strain as Eq. (19)

$$\tilde{u} = \frac{K_\psi^1 - 1}{K_\psi^1 + 1}\rho + \frac{2}{K_\psi^1 + 1}\rho^{-K_\psi^1} \tag{18}$$

$$\tilde{\varepsilon}_\theta^p = \tilde{\varepsilon}_\theta - \tilde{\varepsilon}_{\theta e} = \frac{\tilde{u}}{\rho} - 1 = \frac{2}{K_\psi^1 + 1}\left(\rho^{-(K_\psi^1+1)} - 1\right) \tag{19}$$

Notice that the normalized tangential plastic strain, serving as the softening parameter in this paper, should equal to α at the S–R interface ($\rho = \rho_s$). Therefore, an interesting and important feature comes out that ρ_s (i.e. the ratio of R_s to R_e) is a constant that depends only on the properties of rock mass itself

$$\rho_s = \left(\frac{2}{\alpha K_\psi^1 + \alpha + 2}\right)^{\frac{1}{K_\psi^1+1}} \tag{20}$$

On the other hand, the stress states in the softening region should satisfy the Mohr–Coulomb failure criterion Eq. (12), and meanwhile verify the equilibrium condition formulated by Eq. (21)

$$\frac{d\tilde{\sigma}_r}{d\rho} + \frac{\tilde{\sigma}_r - \tilde{\sigma}_\theta}{\rho} = 0 \tag{21}$$

Associating these two equations with the softening parameter $\tilde{\varepsilon}_\theta^p$ obtained from Eq. (19), the equilibrium equation in the softening region can be derived as

$$\frac{d\tilde{\sigma}_r}{d\rho} + (1 - K_p)\frac{\tilde{\sigma}_r}{\rho} = \frac{\tilde{\sigma}_c^1 + \tilde{\sigma}_c^\delta}{\rho} - \frac{\tilde{\sigma}_c^\delta}{\rho^{K_\psi^1+2}} \tag{22}$$

where $\tilde{\sigma}_c^\delta = 2(\tilde{\sigma}_c^1 - \tilde{\sigma}_c^2)/(\alpha K_\psi^1 + \alpha)$. Solving the differential equation with its boundary condition of $\tilde{\sigma}_r(1) = \tilde{\sigma}_{re}$, the distribution of the normalized radial stress in the softening region can be expressed as

$$\tilde{\sigma}_r = \frac{\tilde{\sigma}_c^1 + \tilde{\sigma}_c^\delta}{1 - K_p} + \frac{\tilde{\sigma}_c^\delta}{K_\psi^1 + K_p}\rho^{-(K_\psi^1+1)} + \left(\tilde{\sigma}_{re} - \frac{\tilde{\sigma}_c^\delta}{1 - K_p} - \frac{\tilde{\sigma}_c^\delta(1 + K_\psi^1)}{(1 - K_p)(K_\psi^1 + K_p)}\right)\rho^{K_p - 1} \tag{23}$$

Since that ρ_s is a constant only depending on the properties of rock mass, while substituting ρ_s for ρ in the above solutions, the normalized states at the S–R interface (e.g. $\tilde{\sigma}_{rs}, \tilde{\varepsilon}_{rs}, \tilde{u}_s$) also come out as constants, just as their counterparts at the E-S interface. They serve as important boundary conditions for further analyses in residual region.

The analyses in residual region are similar to those in softening region. The displacement compatibility equation and the equilibrium equation are formulated as follows, similar to their counterparts referring to as Eqs. (18) and (22)

$$\frac{d\tilde{u}}{d\rho} + K_\psi^2 \frac{\tilde{u}}{\rho} = \tilde{\varepsilon}_{rs} + K_\psi^2 \tilde{\varepsilon}_{\theta s} = K_\psi^2(1 + \alpha) - (1 + \alpha K_\psi^1) \tag{24}$$

$$\frac{d\tilde{\sigma}_r}{d\rho} + (1 - K_p)\frac{\tilde{\sigma}_r}{\rho} = \frac{\tilde{\sigma}_c^2}{\rho} \tag{25}$$

Solving these governing equations with their boundary conditions at the S–R interface, i.e. $\tilde{u}(\rho_s) = \tilde{u}_s$ and $\tilde{\sigma}_r(\rho_s) = \tilde{\sigma}_{rs}$, the normalized displacement and stress distributions in the residual region can be expressed as

$$\tilde{u} = \frac{C_0}{K_\psi^2 + 1}\rho + \left(\tilde{u}_s \rho_s^{K_\psi^2} - \frac{C_0 \rho_s^{1+K_\psi^2}}{K_\psi^2 + 1}\right)\rho^{-K_\psi^2} \tag{26}$$

$$\tilde{\sigma}_r = \frac{\tilde{\sigma}_c^2}{1 - K_p} + \left(\tilde{\sigma}_{rs}\rho_s^{1-K_p} - \frac{\tilde{\sigma}_c^2 \rho_s^{1-K_p}}{1 - K_p}\right)\rho^{K_p - 1} \tag{27}$$

where $C_0 = K_\psi^2(1 + \alpha) - (1 + \alpha K_\psi^1)$.

On the occasion of $\tilde{\sigma}_{rs} < \tilde{P}_i < \tilde{\sigma}_{re}$, the softening region will occur in the surrounding rock mass (i.e. $\rho_s < \rho_a < 1$), and ρ_a can be calculated out in such away that set $\tilde{\sigma}_r$ equal to $\tilde{P}_i$ in Eq. (23). On the occasion of $0 < \tilde{P}_i < \tilde{\sigma}_{rs}$, both the softening region and the residual regions will occur (i.e. $\rho_a < \rho_s$), and ρ_a can be calculated out in such a way that set $\tilde{\sigma}_r$ equal to $\tilde{P}_i$ in Eq. (27). After ρ_a is determined, the minified scale R_e can also be determined by $R_e = R_a/\rho_a$. Then all mechanical states in the physical plane can be evaluated by inverse affine transformation from their counterparts in the unit plane.

3.2.3. Plastic analyses in terms of incremental plastic strain

Based on the incremental theory of plasticity, any problem in plasticity first requires a definition of loading path, so that the rates of all mechanical variables can be evaluated by their first-order derivatives with respect to the loading. As for this problem, the loading path refers to as a monotonic decrease of P_i corresponding to the advancing of tunnel face, which to a turn leads to a monotonic

increase of R_e. Therefore, the rates of all mechanical variables can be evaluated equivalently by their first-order derivatives with respect to R_e, rather than P_i.

The plastic analyses in terms of incremental plastic strain presented below are followed with Carranza-Torres and Fairhurst (1999) and Alonso et al. (2003). It is assumed that the total strain rate consists of both an elastic part and a plastic part, which are controlled by Hooke's law and the potential flow rule respectively, as formulated by Eqs. (28)–(30). The relationship between the strain rate and the deformation velocity is rather simple by virtue of axial symmetry and is formulated by Eq. (31).

$$\dot{\varepsilon}_r = \dot{\varepsilon}_r^e + \dot{\varepsilon}_r^p, \quad \dot{\varepsilon}_\theta = \dot{\varepsilon}_\theta^e + \dot{\varepsilon}_\theta^p \tag{28}$$

$$\dot{\varepsilon}_r^e = \frac{1-v}{2G}\dot{\sigma}_r - \frac{v}{2G}\dot{\sigma}_\theta, \quad \dot{\varepsilon}_\theta^e = \frac{1-v}{2G}\dot{\sigma}_\theta - \frac{v}{2G}\dot{\sigma}_r \tag{29}$$

$$\dot{\varepsilon}_r^p = \lambda\frac{\partial g}{\partial \sigma_r} = \lambda, \quad \dot{\varepsilon}_\theta^p = \lambda\frac{\partial g}{\partial \sigma_\theta} = -\lambda K_\psi \tag{30}$$

$$\dot{\varepsilon}_r = \frac{\partial \dot{u}}{\partial r}, \quad \dot{\varepsilon}_\theta = \frac{\dot{u}}{r} \tag{31}$$

Here, v is the Poisson ratio of rock mass, and the rates of all mechanical variables (denoted by dot mark) refer to as their first-order derivatives with respect to R_e. Associating these four equations, eliminating the scalar λ, the displacement compatibility equation in the physical plane can be expressed as

$$\frac{\partial \dot{u}}{\partial r} + K_\psi\frac{\dot{u}}{r} = \frac{(1-v-vK_\psi)}{2G}\dot{\sigma}_r - \frac{(vK_\psi - K_\psi + v)}{2G}\dot{\sigma}_\theta \tag{32}$$

An additional condition is the consistency equation, which implies that the material remains in the plastic state once this state has been achieved.

$$\frac{\partial f}{\partial \sigma_r}\dot{\sigma}_r + \frac{\partial f}{\partial \sigma_\theta}\dot{\sigma}_\theta + \frac{\partial f}{\partial \eta}\dot{\eta} = 0 \tag{33}$$

Applying the affine transformation to the above two equations (expressed in partial derivatives), the displacement compatibility equation and the consistency equation in the unit plane (expressed in ordinary derivatives) can be expressed as Eqs. (34) and (35).

$$\frac{d^2\tilde{u}}{d\rho^2} + K_\psi\frac{d\tilde{u}}{d\rho}\frac{1}{\rho} - K_\psi\frac{\tilde{u}}{\rho^2} = (1-v-vK_\psi)\frac{d\tilde{\sigma}_r}{d\rho} - (vK_\psi - K_\psi + v)\frac{d\tilde{\sigma}_\theta}{d\rho} \tag{34}$$

with its boundary conditions $\tilde{u}(1) = 1, \tilde{\dot{u}}(1) = \tilde{\varepsilon}_{re} = -1$.

$$\frac{\partial \tilde{f}}{\partial \tilde{\sigma}_r}\frac{d\tilde{\sigma}_r}{d\rho} + \frac{d\tilde{f}}{\partial \tilde{\sigma}_\theta} + \frac{d\tilde{\sigma}_\theta}{\partial \rho} + \frac{\partial \tilde{f}}{\partial \tilde{\varepsilon}_\theta^p}\frac{d\tilde{\varepsilon}_\theta^p}{d\rho} = 0 \tag{35}$$

On the other hand, associating the Mohr–Coulomb failure criterion Eq. (12) and the equilibrium condition Eq. (21), the equilibrium equation can be expressed as:

$$\frac{d\tilde{\sigma}_r}{d\rho} + (1-K_p)\frac{\tilde{\sigma}_r}{\rho} = \frac{\tilde{\sigma}_c}{\rho} \tag{36}$$

with its boundary condition $\tilde{\sigma}_r(1) = \tilde{\sigma}_{re}$.

The displacement compatibility equation and the equilibrium equation (together with the failure criterion and the consistency equation) are simultaneous, and can only be solved by numerical method (say the fourth Runge–Kutta method). From their initial states at the E–S interface (known as constants), one can evaluate their states at the sequential positions iteratively, and stop the iteration when $\tilde{\sigma}_r = \widetilde{P}_i$. Then the current position is recorded as ρ_a, and the minified scale can be determined by $R_e = R_a/\rho_a$. Finally, all mechanical states recorded in the unit plane are transformed inversely into their counterparts in the physical plane.

4. Discussions on two categories of theoretical methods

4.1. The discrepancy between two categories of theoretical methods

Both of these two theoretical methods presented above are implemented by VB programming. Then a representative case is studied by these two methods, to illustrate the discrepancy between them. The properties of rock mass employed in this case are listed in the first line of Table 1, the radius of tunnel opening R_a and the inner pressure P_i are set to 5 m and 0 MPa. To validate these two theoretical methods, the representative case is studied identically by numerical simulations (code: FLAC^{3D}), with its necessary parameters listed in the second row of Table 1. The strain-softening constitutive laws in FLAC^{3D} are characterized by friction angle ϕ, cohesion c, dilation angle ψ and a softening parameter η, former three of which may be any functions of softening parameter η (in tabulated form). It is obvious that friction angle, cohesion and dilation angle can be obtained directly from passive coefficient, compression strength and dilation factor, as following relations:

$$K_p = \frac{1+\sin\phi}{1-\sin\phi} \tag{37.1}$$

$$\sigma_c = 2c\sqrt{K_p} \tag{37.2}$$

$$K_\psi = \frac{1+\sin\psi}{1-\sin\psi} \tag{37.3}$$

Table 1
Rock mass properties employed in a representative case

Theoretical methods						
G (MPa)	v	K_p	σ_c^1, σ_c^2 (MPa)	K_ψ^1, K_ψ^2	α	P_0 (MPa)
400	0.25	3	5,3	2.5,1.5	0.5	10
Numerical simulations						
G (MPa)	K (MPa)	ϕ (°)	c^1, c^2 (MPa)	ψ^1, ψ^2 (°)	η_{res}	P_0 (MPa)
400	667	30	1.443, 0.866	25.4, 1.5	0.0078	10

However, the softening parameter η in FLAC^{3D} is defined as: (Itasca, 1997)

$$\delta\eta = \frac{1}{\sqrt{2}}\sqrt{(\delta\varepsilon_1^p - \delta\varepsilon_m^p)^2 + (\delta\varepsilon_m^p)^2 + (\delta\varepsilon_3^p - \delta\varepsilon_m^p)^2} \quad (38.1)$$

where $\delta\varepsilon_m^p = (\delta\varepsilon_1^p + \delta\varepsilon_3^p)/3$. Corresponding to this case, the shift point of softening parameter in FLAC^{3D} that distinguishes residual region from softening region can be evaluated by:

$$\eta_{res} = \frac{\varepsilon_{\theta e}}{\sqrt{6}}\sqrt{(2\alpha + \alpha K_\psi^1)^2 + (\alpha - \alpha K_\psi^1)^2 + (\alpha + 2\alpha K_\psi^1)^2} \quad (38.2)$$

The stress and displacement distributions in the surrounding rock mass that are calculated by two theoretical methods (denoted by the solid and dashed lines) are depicted in Fig. 4. The results from the numerical simulations (denoted by the cross marks) are also depicted in this figure. For the most part, the stress distributions calculated by these two methods fit each other exactly, and the convex point and the concave point on the σ_θ/P_0 curve denote the positions of the E–S and the S–R interfaces in this case. However, there exists a considerable discrepancy between these two methods in depicting the displacement distribution of the plastic region. The results from the numerical simulations, indubitably, fit the rigorous semi-analytical method but not the simplified one. The significant difference between these two methods lies in the different assumptions on the displacement compatibility equation, as referred to Eqs. (14) and (28), i.e. whether or not to take the unloading process into account in displacement calculation. The difference is elucidated schematically in Fig. 5.

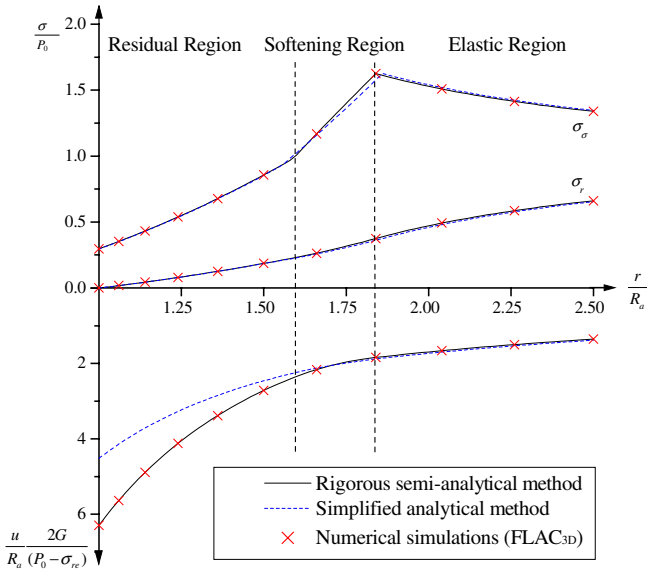

Fig. 4. The stress and displacement distributions in the surrounding rock mass.

In Fig. 5a, the fixed points B and C denote the stress states at the E–S and S–R interfaces, which are constants and independent of their positions. Stress states in line BC and line CD are governed by the stress governing equations, referring to Eqs. (22), (25) in the simplified method and Eq. (36) in the rigorous one. The moving point P represents the stress state at tunnel wall, which moves along the path of ABCD, corresponding to the decreasing of inner pressure. Therefore, sthe bold line from A to P represents the stress states in the surrounding rock mass after excavation.

Fig. 5b illustrates the evolution of the plastic region with the decreasing of P_i, which corresponds to the advancing of the tunnel face. In order to evaluate the displacement distribution at the current stage (say the tth stage where $P_i = P_i^{(t)}$), the rigorous method evaluates the displacement distribution iteratively from the nth stage where $P_i = \sigma_{re}$ to the current stage, according to the displacement compatibility equation Eq. (34). The simplified method, on the contrary, does not take the influence of the unloading process into account and evaluates the displacement distribution

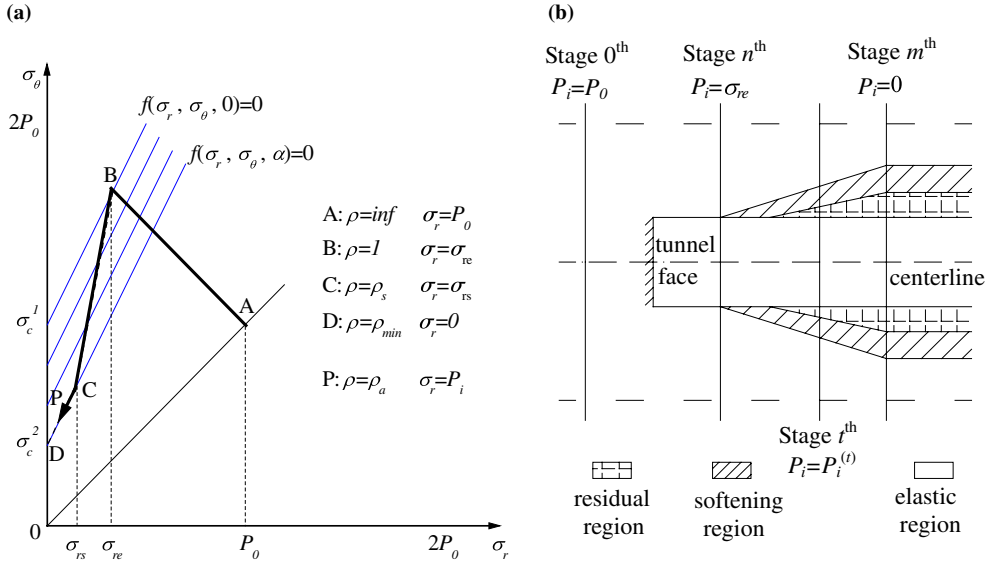

Fig. 5. (a) Stress states in the surrounding rock mass after excavation and (b) evolution of the plastic region according to the unloading process.

directly, according to the current inner pressure $P_i^{(t)}$ and the displacement compatibility equations Eqs. (17) and (24).

The simplified method based on total plastic strain was particularly represented by Brown et al. (with Hoek–Brown failure criterion, 1983) and Jiang (with Mohr–Coulomb failure criterion, 1993). The rigorous method based on incremental plastic strain was particularly represented by Detournay (with Mohr–Coulomb failure criterion, 1986) and Carranza-Torres and Fairhurst (with Hoek–Brown failure criterion, 1999). However, the discrepancy between them has never been noticed and reported. The following discussion estimates the error caused by the simplified one.

4.2. Parameter studies and discussions

Taking the illustrative case presented above as the basic case, changing the mechanical properties of rock mass, some derivative cases are studied in this section for two purposes: to illustrate the influence of rock mass properties on the ground reaction and to estimate the error of the simplified method in displacement calculation. First, the error of the simplified method in the tunnel convergence calculation is defined as:

$$\mathrm{err} = \frac{u_a^{(\mathrm{rig})} - u_a^{(\mathrm{sim})}}{u_a^{(\mathrm{rig})}} \tag{38}$$

where $u_a^{(\mathrm{rig})}$ and $u_a^{(\mathrm{sim})}$ are the tunnel convergences (namely the released displacements at tunnel wall) evaluated by the rigorous and the simplified methods. Apparently, The error will reach its maximum $\mathrm{err}_{\max}$ on the occasion of $P_i = 0$.

Three groups of derivative cases with different K_p, $\sigma_c^1(\sigma_c^2)$ and $K_\psi^1(K_\psi^2)$ are studied by the two theoretical methods, and their ground reaction curves are depicted in Figs. 6–8. Both of these two theoretical methods show the same tendency that the strength characters of rock mass, K_p and $\sigma_c^1(\sigma_c^2)$, influence the range of the plastic region significantly, which in turn influence the tunnel convergence dramatically, as illustrated in Figs. 6 and 7. On the contrary, the dilation factor of rock mass $K_\psi^1(K_\psi^2)$ does not influence the range of the plastic region, but also influences the tunnel convergence to some extent, as illustrated in Fig. 8. While focusing on the error of the simplified method in displacement calculation, it will increase monotonically with the decreasing of $\sigma_c^1(\sigma_c^2)$ and the increasing of $K_\psi^1(K_\psi^2)$, but seems independent of K_p. According to parameter studies, the $\mathrm{err}_{\max}$ caused by the simplified method is estimated to range from 20% to 40% on common conditions.

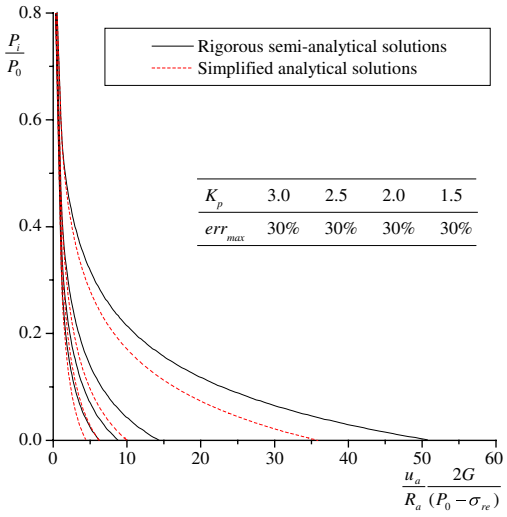

Fig. 6. The influence of K_p on GRC.

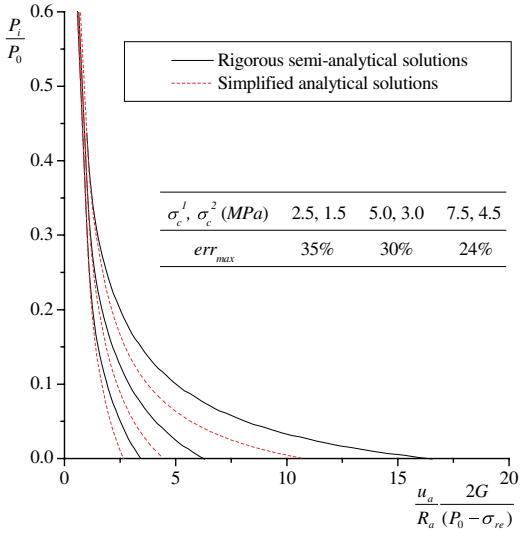

Fig. 7. The influence of σ_c^1, σ_c^2 on GRC.

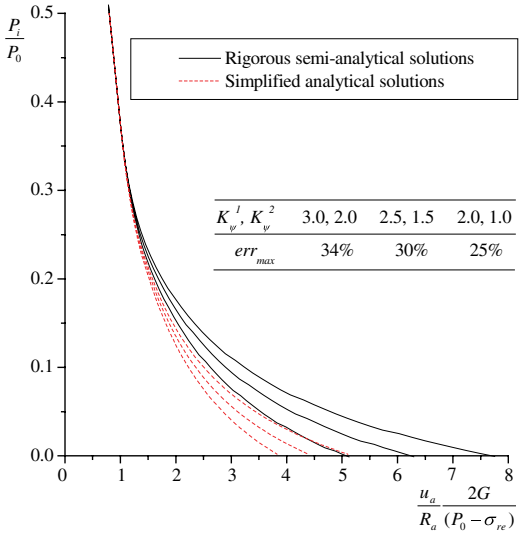

Fig. 8. The influence of K_ψ^1, K_ψ^2 on GRC.

5. Conclusions

Ground reaction analyses for the conventional tunnelling excavation have been discussed by numerous researchers, with different rock mass constitutive laws, different

excavation conditions and different approaches. Particularly, based on the axial symmetrical plane strain assumption, the analytical (or semi-analytical) ground reaction analyses attracted most attentions, because it serves as one of the three basic components in the convergence confinement method and play an important role in the design of tunnel support system. The available methods, although distinguished from different constitutive laws, can be generally divided into two categories according to their treatments for the plastic strain. One is the simplified method in terms of total plastic strain, and the other is the rigorous method in terms of incremental plastic strain.

Based on the rationales proposed by former researchers, given that the rock mass satisfies the Mohr–Coulomb failure criterion and exhibits strain-softening behaviors, these two categories of theoretical methods are derived respectively in this paper. The significant difference between them lies in the different assumptions on the displacement compatibility equation in terms of total or incremental plastic strain, in other words, whether or not to consider the unloading process in displacement calculation. Through an illustrative case, it is revealed that although the stress distributions evaluated by these two methods fit each other well, there exists a considerable discrepancy between them in depicting the displacement distribution of plastic region. It is indubitable that the rigorous semi-analytical method reflects the nature of tunnel excavation more realistically, and the simplified one underestimates the displacement released in the plastic region of the surrounding rock mass.

The simplified method can only be used in predicting the range of plastic region and the stress distribution in surrounding rock mass, but is estimated to have an error in evaluating the tunnel convergence, which ranges from 20% to 40% on common conditions.

Acknowledgement

The author would like to thank Professor Huang, Vice Dean of the Graduate School of Tongji University, for his valuable comments and suggestions to this paper.

References

Alonso, E., Alejano, L., Varas, F., Fdez-Manin, G., Carranza-Torres, C., 2003. Ground reaction curves for rock masses exhibiting strain-softening behaviour. Int. J. Numer. Anal. Meth. Geomech. 27 (13), 1153–1185.

Brown, E., Bray, J., Landayi, B., Hoek, E., 1983. Ground response curves for rock tunnels. ASCEJ. Geotech. Eng. Div. 109 (1), 15–39.

Carranza-Torres, C., Fairhurst, C., 1999. The elasto-plastic response of underground excavations in rock masses that satisfy the Hoek–Brown failure criterion. Int. J. Rock Mech. Min. Sci. 36 (6), 777–809.

Carranza-Torres, C., Fairhurst, C., 2000. Application of convergence-confinement method of tunnel design to rock masses that satisfy the Hoek–Brown failure criterion. Tunnelling and Underground Space Technology 15 (2), 187–213.

Detournay, E., 1986. Elastoplastic model of a deep tunnel for a rock with variable dilatancy. Rock Mech. Rock Engng. 1986 (19), 99–108.

Graziani, A., Boldini, D., Ribacchi, R., 2005. Practical Estimate of Deformations and Stress Relief Factors for Deep Tunnels Supported by Shotcrete. Rock Mech. Rock Engng. 38 (5), 345–372.

Hill, R., 1950. The Mathematical Theory of Plasticity. Oxford University Press, London.

Hudson, J., Harrison, J., 1997. Engineering Rock Mechanics. Pergamon, London.

Itasca Consulting Group, 1997, FLAC^{3D}, Fast Lagrange Analysis of Continua in 3 Dimensions, Version 2.0, User Manual. Minneapolis.

Jiang, Y., 1993. Theoretical and experimental study on the stability of deep underground opening. Ph.D. Thesis, Kyushu University.

Jiang, Y., Yoneda, H., Tanabashi, Y., 2001. Theoretical estimation of loosening pressure on tunnels in soft rocks. Tunnelling and Underground Space Technology 16 (2), 99–105.

Oreste, P., 2003. Analysis of structural interaction in tunnels using the convergence-confinement approach. Tunnelling and Underground Space Technology 18 (4), 347–363.

Oreste, P., Peila, D., 1996. Radial passive rockbolting in tunnelling design with a new convergence confinement model. Int. J. Rock Mech. Min. Sci. Geomech. Abstr. 33 (5), 443–454.

Panet, M., Guenot, A., 1982. Analysis of convergence behind the face of a tunnel. In: Proc. Tunnelling '82, London, 197–204.

Timoshenko, S., Goodier, J., 1970. Theory of Elasticity. McGraw-Hill, New York.

Tonon, F., Amadei, B., 2002. Effect of elastic anisotropy on tunnel wall displacements behind a tunnel face. Rock Mech. Rock Engng. 35 (3), 141–160.

Varas, F., Alonso, E., Alejano, L., Fdez-Manin, G., 2005. Study of bifurcation in problem of unloading a circular excavation in a strain-softening material. Tunnelling and Underground Space Technology 20 (4), 311–322.